

# Soluble PD-1 ligands regulate T-cell function in Waldenstrom macroglobulinemia

Shahrzad Jalali, Tammy Price-Troska, Jonas Paludo, Jose Villasboas, Hyo-Jin Kim, Zhi-Zhang Yang, Anne J. Novak, and Stephen M. Ansell

Division of Hematology and Internal Medicine, Mayo Clinic, Rochester, MN

## Key Points

- Cytokines in the BM microenvironment regulate PD-1 ligand expression and secretion in WM.
- Secreted PD-1 ligands modulate T-cell function in WM.

Although immune checkpoint molecules regulate the progression of certain cancers, their significance in malignant development of Waldenstrom macroglobulinemia (WM), an incurable low-grade B-cell lymphoma, remains unknown. Recently, cytokines in the bone marrow (BM) microenvironment are shown to contribute to the pathobiology of WM. Here, we investigated the impact of cytokines, including interleukin-6 (IL-6) and IL-21, on immune regulation and particularly on the programmed death-1 (PD-1) and its ligands PD-L1 and PD-L2. We showed that IL-21, interferon  $\gamma$ , and IL-6 significantly induced PD-L1 and PD-L2 gene expression in WM cell lines. Increased PD-L1 and PD-L2 messenger RNA was also detected in patients' BM cells. Patients' nonmalignant BM cells, including T cells and monocytes, showed increased PD-L1, but minimal or undetectable PD-L2 surface expression. There was also very modest PD-L1 and PD-L2 surface expression by malignant WM cells, suggesting that ligands are cleaved from the cell surface. Levels of soluble ligands were higher in patients' BM plasma and blood serum than controls. Furthermore, IL-21 and IL-6 increased secreted PD-L1 in the culture media of WM cell lines, implying that elevated levels of soluble PD-1 ligands are cytokine mediated. Soluble PD-1 ligands reduced T-cell proliferation, phosphorylated extracellular signal-regulated kinase and cyclin A levels, mitochondrial adenosine triphosphate production, and spare respiratory capacity. In conclusion, we identify that soluble PD-1 ligands are elevated in WM patients and, in addition to surface-bound ligands in WM BM, could regulate T-cell function. Given the capability of secreted forms to be bioactive at distant sites, soluble PD-1 ligands have the potential to promote disease progression in WM.

## Introduction

Waldenstrom macroglobulinemia (WM) is an uncommon low-grade B-cell lymphoma characterized by a lymphoplasmacytic infiltrate within the bone marrow (BM) and by increased synthesis and accumulation of monoclonal immunoglobulin M (IgM) in the serum, which increases the risk of hyperviscosity in the affected patients.<sup>1,2</sup> Despite advancements in understanding the biology of WM<sup>3</sup> and introduction of novel therapeutic interventions,<sup>4</sup> the disease still remains incurable. Recent studies indicate that the underlying molecular mechanisms contributing to the pathogenesis of WM are attributed not only to the genomic aberrations of malignant cells<sup>5</sup> but also to the complex signaling events arising from the interaction of malignant cells with the components of BM milieu.<sup>6,7</sup> Chromosomal deletion, recurrent somatic mutations, and copy-number alterations are frequently found in WM tumor cells.<sup>8</sup> However, next-generation whole-genome sequencing analysis of the lymphoplasmacytic lymphoma cells has revealed prevalent somatic mutations in myeloid differentiation factor 88 (MYD88) and CXCR4 found in ~90% and 40% of WM patients, respectively.<sup>5,8-10</sup> Mutant MYD88, an adaptor protein downstream of Toll-like (TLR) and interleukin-1 (IL-1) receptors, forms a complex with Bruton tyrosine kinase and

induces constitutive activation of NF- $\kappa$ B resulting in increased proliferation and survival of the WM cells.<sup>11</sup> In addition, mutations in CXCR4 are found to constitutively activate phosphatidylinositol 3-kinase/Akt and extracellular signal-regulated kinase (ERK) signaling pathways, enhancing survival of the WM cells.<sup>12</sup>

Although genomic alteration in WM cells skew the signaling pathways toward more of a proliferative and aggressive phenotype, recent studies highlight that the BM microenvironment, including both cellular and noncellular compartments, plays a significant role in mediating increased proliferation and IgM secretion by WM cells.<sup>6,7,13</sup> Analysis of cytokine and chemokine expression in healthy subjects and WM patients has revealed that certain chemokines and cytokines including granulocyte colony-stimulating factor (G-CSF), soluble IL-2 receptor (sIL-2R), CCL5, IL-6, IL-21, macrophage inflammatory protein-1 $\alpha$ , and B-lymphocyte stimulator are significantly increased in the serum and BM of the WM patients.<sup>14-18</sup> Elevated levels of IL-21, IL-6, and B-lymphocyte stimulator have been shown to increase proliferation and survival of WM cells and contribute to IgM secretion.<sup>14,16,19</sup> Altered cytokine expression can regulate the signaling events controlling immune responses within the BM microenvironment,<sup>20,21</sup> however, to date, there are no data available on whether changes in the cytokine composition of the WM BM could have an impact on immune checkpoint molecules and regulate T-cell function.

The programmed death-1 (PD-1) receptor and the 2 naturally occurring ligands PD-L1 and PD-L2 belong to B7 family members of immune checkpoint molecules that negatively regulate the activation and proliferation of T lymphocytes. Although the interaction of PD-1 with its ligands is important in maintaining immune tolerance, reduced T-cell activity could provide an opportunity for tumor cells to evade immune responses.<sup>22-24</sup> Increased PD-1 or PD-L1 expression on the cell surface of tumors cells has been reported in hematological cancers<sup>25</sup> as well as solid tumors including melanoma,<sup>26,27</sup> lung,<sup>28</sup> breast,<sup>29</sup> ovarian,<sup>30</sup> and bladder cancers.<sup>31</sup> Monoclonal antibodies to target PD-1 or PD-L1 are routinely being used for the treatment of these patients and are associated with increased response rates and survival.<sup>32-34</sup> However, to date, there are no data available on how the BM microenvironment modulates PD-1 and its ligands and thus contributes to the pathophysiology of WM.

The goal of this study was to explore whether cytokines in the WM BM microenvironment could modulate the expression of immune checkpoint molecules, PD-1 and the ligands PD-L1 and PD-L2, and therefore regulate the immune function and contribute to WM pathogenesis.

## Materials and methods

### Cell culture and reagents

The WM cell lines BCWM.1 (a gift from Steven Treon, Dana-Farber Cancer Institute, Boston, MA) and MWCL-1 (established in our laboratory) were used in this study. All cells were maintained in RPMI 1640 (Invitrogen) supplemented with 50 U/mL penicillin G, 10  $\mu$ g/mL streptomycin, 10% heat-inactivated fetal bovine serum (FBS), 1 mM sodium pyruvate (Sigma-Aldrich), and 1% minimal essential medium nonessential amino acids (Sigma-Aldrich) at 37°C with 5% CO<sub>2</sub>. Recombinant human IL-6, IL-21, interferon  $\gamma$  (IFN $\gamma$ ), and CCL5 were obtained from PeproTech.

### Patients' specimens

All samples were received from WM patients and normal subjects under Mayo Clinic institutional review board approval and in

accordance with the Declaration of Helsinki. Both symptomatic and asymptomatic (smoldering) WM samples were included in this study. WM was defined as the presence of circulating IgM monoclonal protein of any size with  $\geq 10\%$  BM infiltration with lymphoplasmacytic cells. Smoldering WM was defined as the presence of serum IgM monoclonal protein level  $\geq 3$  g/dL and/or BM containing  $\geq 10\%$  of lymphoplasmacytic lymphoma, with no evidence of end-organ damage. WM samples with mutant or wild-type MyD88 were both included in this study. The BM biopsies were obtained from consented WM patients ( $n = 28$ ). Control BM specimens ( $n = 20$ ) were collected from the patients who had undergone hip replacement surgery. Cellular fractions were separated from noncellular (BM plasma) fraction by centrifugation at 2500 rpm for 10 minutes. BM plasmas were immediately snap-frozen in liquid nitrogen and stored in  $-80^{\circ}\text{C}$  for future analysis. BM cells were first ammonium-chloride-potassium (ACK) lysed to remove red blood cells and then centrifuged at 400g for 5 minutes. Cell pellets were resuspended in RPMI, passed through 70- $\mu\text{m}$  filters, washed, and subsequently used for isolation of CD19<sup>+</sup>/138<sup>-</sup> and CD19<sup>+</sup>/138<sup>+</sup> cell populations using the fully automated RoboSep 20 000 cell separation system and EasySep human positive selection kits for CD19 and CD138 (StemCell Technologies). Serum samples were obtained from WM patients ( $n = 52$ ) and matched normal donors ( $n = 20$ ) and used for soluble PD-L1 and PD-L2 detection.

### RT-PCR analysis

RNA was extracted from CD19<sup>+</sup>/138<sup>+</sup> and CD19/138<sup>-</sup> cells using the miRNeasy Mini kit (Qiagen), the same day after sample delivery. Complementary DNA (cDNA) synthesis and subsequent real-time polymerase chain reaction (RT-PCR) analysis were performed at the same time, on all collected patients' samples. WM cell lines were treated with 100 ng/mL IFN $\gamma$ , CCL5, IL-21, G-CSF, or 50 ng/mL IL-6 for 3 days. Control (vehicle-treated) cells did not receive cytokines. All of the cells were next collected and subjected to RNA isolation, cDNA synthesis, and RT-PCR analysis at the same time. In summary, 500  $\mu\text{g}$  of isolated RNA was used for cDNA synthesis by SuperScript III First-Strand Synthesis SuperMix (Invitrogen) followed by real-time PCR analysis using Hot starTaq Master Mix (Qiagen) and predesigned probes and primers (all from Integrated DNA Technologies [IDT]) for PD-1 (probe, 5'-/56 FAM/CGG CCA GGA/ZEN/TGG TTC TTA GAC TCC/3IABkFQ/-3'; primer 1, 5'-GGC GGT GCT ACA ACT GG-3'; primer 2, 5'-AGG GCT GGG GAG AAG GT-3'), PD-L1 (probe, 5'-/56-FAM/AGC ATT GGA/ZEN/ACT TCT GAT CTT CAA GCA GG/3IABkFQ/-3'; primer 1, 5'-GGC ATC CAA GAT ACA AACTCA AAG-3'; primer 2, 5' CTT CCT CTT GTC ACG CTC AG-3'), PD-L2 (probe, 5'-/56-FAM/AGC ACT TGT T/ZEN/CAC TTC CCT CTT TGT TGT/3IABkFQ/-3'; primer 1, 5'-CAA AAG CTG TAT TCT TCA AAA GAC AC-3'; primer 2, 5'-AGA TGT CAT ATC AGG TCA CCC T-3'), and RPLP0 (probe, 5/HEX/CCC TGT CTT/ZEN/CCC TGG GCA TCA C/3IABkFQ/-3'; primer 1, 5'-TTA AAC CCT GCG TGG CAATTA AAC CCT GCG TGG CAA-3'; 5'-GTC TGC TCC CAC AAT GAA AC-3') as a housekeeping gene. Amplification of the genes was run on a Bio-Rad CFX96 Real-Time System and the relative gene expression, normalized to housekeeping gene, was quantified using the 2<sup>- $\Delta\Delta\text{CT}$</sup>  method (where CT is the cycle threshold) and data were reported as mean plus or minus standard error (SE).

### Cell transfection

WM cell lines, MWCL-1 and BCWM.1, and a control embryonic kidney cell line, HEK293, were transfected with PD-L1 and PD-L2

coding sequence using the pLEX-MCS Inducible Expression System (Open Biosystems). Each gene of interest was created by RT-PCR. Primers were designed to incorporate restriction sites *Xho*I (5') and *Age*I (3') for PD-L1 and *Bam*HI (5') and *Age*I (3') for PD-L2 vectors, then ligated into the pLEX-MCS vector using T4 DNA Ligase (New England Biolabs). The plasmid lentivirus was amplified using DH5 $\alpha$  (*Escherichia coli*) competent cells. The virus was produced according to the manufacturer's instructions and introduced into MWCL-1, BCWM.1, and HEK293 cell lines. After 5 days of exposure to the virus, the transfected cells were selected using puromycin. Fourteen days posttransfection, cells were screened for the expression of PD-L1 and PD-L2 by flow cytometry.

### Flow cytometry

To detect cell surface expression of PD-1, PD-L1, and PD-L2 on CD19<sup>+</sup>/138<sup>+</sup> or CD19/138<sup>-</sup> cell populations and to confirm the overexpression of PD-L1 and PD-L2 on the cell surface of transfected WM cell lines, cells were first stained with fixable viability dye eFlour 780 (eBioscience) and then incubated with fluorescent-conjugated mouse anti-human antibodies including PD-1–peridinin chlorophyll protein complex–Cy 5.5 (BD Biosciences), PD-L1–BV421, PD-L2–phycoerythrin (PE) (Biolegend), or fluorescent-conjugated mouse IgG1 isotype control for 45 minutes at room temperature. The BM CD19/138<sup>-</sup> cell population was also stained with CD14–PE–cy7, CD15–fluorescein isothiocyanate, CD3–fluorescein isothiocyanate, CD56–PE–cy7 to identify and gate on viable T cells, monocytes, natural killer (NK) cells, and neutrophils, respectively. Stained cells were analyzed on a Becton Dickinson (BD) FACSCanto II and data were processed by FlowJo software (V10.4).

### T-cell isolation and proliferation assay

T cells were isolated from peripheral blood mononuclear cells (PBMCs). Briefly, whole blood was collected from normal donors and mixed with phosphate-buffered saline in a 1:5 ratio. The mixture was overlaid on top of 15 mL of Ficoll and centrifuged at 400g for 30 minutes. Mononuclear cells were gently collected from the interface between Ficoll and plasma layer, washed with phosphate-buffered saline, and ACK lysed to remove red blood cells. Isolated PBMCs were used to extract T cells using RoboSep and a T-cell isolation kit (T-cell negative selection kit; StemCell Technologies). T-cell proliferation was assessed using <sup>3</sup>H–Thymidine (<sup>3</sup>H]TdR) incorporation. Briefly, T cells were mixed with cell-free media collected from control empty vector (EV), PD-L1–, or PD-L2–transfected WM cell lines and plated at a density of 1 × 10<sup>5</sup>/100  $\mu$ L per well on 96-well plates coated with 5  $\mu$ g/mL OKT3 (BioLegend) in the presence of CD28 (BD Biosciences). Cells were cultured for 3 days, labeled with 1  $\mu$ Ci per well of [<sup>3</sup>H]TdR for 18 hours, and harvested; incorporation of [<sup>3</sup>H]TdR was measured using MicroBeta scintillation counter (PerkinElmer).

### Immunohistochemistry

Formalin-fixed paraffin-embedded BM biopsy sections were obtained from control and WM patients. The sections were deparaffinized in Xylene, rehydrated in graded ethanol, incubated in 3% hydrogen peroxide (H<sub>2</sub>O<sub>2</sub>) in methanol for 10 minutes to block endogenous peroxidase, followed by heat-induced epitope retrieval using 1 mM EDTA (pH 8) for 30 minutes. After blocking with 5% goat serum, the sections were first incubated with primary antibodies for PD-1 (Biacore Medical), PD-L1 and PD-L2 (Spring Bioscience) for 30 minutes and next by secondary antibodies and streptavidin (30 minutes each). The

staining was then detected using Vectastain ABC and diaminobenzidine, counterstained with Meyer hematoxylin, dehydrated with graded ethanol and Xylene, and mounted. All slides were scanned using an Olympus Ax70 microscope.

### ELISA

Normal and WM BM biopsies were processed to isolate BM plasma from cellular component by centrifugation at 2500 rpm for 10 minutes. Peripheral blood serum samples were also obtained from normal donors and WM patients. WM cell lines were treated with cytokines for 3 days and cell-free media were collected. BCWM.1 cells were stimulated with 50 ng/mL IL-6 or 100 ng/mL IL-21, in the presence or absence of 0.5  $\mu$ M STATTIC (STAT3 inhibitor) or 1  $\mu$ M CP690550 (JAK inhibitor), respectively. Soluble PD-L1 and PD-L2 levels in the patients' BM plasma and peripheral serum, as well as in the media of cytokine-treated WM cell lines, were determined using human PD-L1 (Abcam) and PD-L2 (R&D Systems) enzyme-linked immunosorbent assay (ELISA) kits according to the provider's instruction.

### Western blot analysis

To detect soluble PD-1 ligands in the media of HEK293 and WM cell lines, transfected cells overexpressing PD-L1 or PD-L2 were serum-starved for 2 days. Culture media were collected and concentrated using Amicon Ultra-15 10K Centrifugal Filter devices (Millipore) and subjected to protein assay using a protein assay kit (Bio-Rad). To show any change in T-cell cycle and survival protein expression in response to soluble PD-L1 and PD-L2, transfected HEK293 and WM cell lines (1 × 10<sup>6</sup> cells/mL) were cultured in their corresponding media containing growth factors for 2 days. Cell-free media were then collected and added to isolated T cells from PBMCs and the mixture was cultured for 2 more days. T cells were then lysed using radioimmunoprecipitation assay cell lysis buffer and protein concentration was determined. Samples containing 30  $\mu$ g of total protein, including concentrated media and cell lysates, were run on 10% sodium dodecyl sulfate–polyacrylamide gel electrophoresis, transferred to nitrocellulose membrane (Bio-Rad), and probed with primary antibodies for PD-L1, PD-L2 (Abcam), cyclin A, cyclin D1, phospho-ERK, and actin (Cell Signaling) and horseradish peroxidase–conjugated secondary antibodies (Bio-Rad). Membranes were then incubated with Supersignal chemiluminescent substrates (Thermo Fischer Scientific) and the bands were captured using radiograph films.

### OCR measurement

T cells were isolated from PBMCs, cultured in RPMI 1640 containing 10% FBS, and stimulated with Dynabeads Human T-Activator CD3/CD28 (Thermo Fischer Scientific) for 3 days. MWCL-1 cells expressing control (EV), PD-L1 or PD-L2 were cultured at RPMI with 10% FBS for 3 days and the cell free–conditioned media were collected. T cells were then incubated with collected condition media for an additional 3 days and oxygen consumption rate (OCR) was analyzed using the Cell Mito Stress kit (Agilent) and the Seahorse XFp Extracellular Flux Analyzer (Seahorse Bioscience). Briefly, T cells were resuspended in Agilent Seahorse XF Base Medium RPMI without phenol red, plated onto Seahorse cell plates (2.5 × 10<sup>5</sup> cells per well), and incubated in a CO<sub>2</sub>-free humidified 37°C incubator for 1 hour. Mitochondrial respiration function was assessed by sequential injection of electron transport chain modulators, including 1  $\mu$ M oligomycin, 1  $\mu$ M carbonyl cyanide-4 phenylhydrazone, and 1  $\mu$ M rotenone/antimycin A, over an 80-minute period. The analyzed stress test

parameters were exported from the analyzer and the graphs were prepared by GraphPad Prism (V6) software.

## Statistical analysis

Unpaired Student *t* test analysis was used to compare differences between control untreated and cytokine-treated cell lines. The Wilcoxon paired nonparametric test was used to examine the significant differences between mean values of patients and normal groups. All analyses were performed on the GraphPad Prism (V6) software, and data were reported as mean plus or minus SE.

## Results

### Effect of cytokine treatment on PD-1, PD-L1, and PD-L2 expression by WM cell lines

Analysis of cytokine levels in the WM patients has previously shown that IL-6, G-CSF, IL-21, and CCL5 cytokines are significantly elevated within WM BM microenvironment.<sup>14</sup> To examine whether these cytokines can regulate the expression of the immune checkpoint molecule PD-1 and its ligands in vitro, we treated WM cell lines, BCWM.1 and MWCL-1, with 100 ng/mL of either IL-21, IFN $\gamma$ , G-CSF, CCL5 or 50 ng/mL IL-6 for 72 hours (Figure 1). RT-PCR data (Figure 1A-B) showed that PD-1 messenger RNA (mRNA) was increased by G-CSF and IFN $\gamma$  in only BCWM.1 cells and remained unchanged in other treatment settings. The effect of cytokines on PD-L1 gene expression was similar in both cell lines. IL-21, IL-6, and IFN $\gamma$  significantly increased PD-L1 gene expression, whereas CCL5 and G-CSF did not show any effect when compared with control untreated cells. In contrast to PD-L1, cytokine-mediated PD-L2 gene expression was cell-line specific, in that IL-21 and IL-6 increased PD-L2 expression in only MWCL-1 line (Figure 1A-B). Altogether, these results suggest that cytokines can modulate expression of PD-1 ligands in WM cells. Furthermore, the pattern of cytokine-induced PD-L1 gene expression appeared to be consistent in both cell lines examined in this study. We then analyzed surface expression of both ligands using flow cytometry (Figure 1C). We found that only IL-21-treated BCWM.1 cells showed increased PD-L1 surface expression compared with control untreated cells and in contrast to the cytokine-treated gene expression data (Figure 1A-B), we could not detect any upregulation of PD-L1 (Figure 1C) or PD-L2 (data not shown) in any of the other treatment settings.

### PD-1, PD-L1, and PD-L2 expression by CD19<sup>-</sup>/138<sup>-</sup> and CD19<sup>+</sup>/138<sup>+</sup> cell population isolated from WM and normal BM

Altered PD-1 ligands expression following cytokine treatment in WM cell lines prompted us to examine the gene and protein expression of PD-1 and its ligands in the cells of BM samples and explore whether perturbation in the cytokine composition of BM microenvironment in WM could have changed the expression pattern of these molecules. To address this, BM biopsies were collected from WM patients and the lymphoplasmacytic cells positive for CD19 and CD138 markers (CD19<sup>+</sup>/138<sup>+</sup>) were separated from the rest of the BM microenvironment (CD19<sup>-</sup>/138<sup>-</sup>). Equivalent cell populations were also collected from normal BM samples, and RT-PCR analysis was performed to detect PD-1, PD-L1, and PD-2 gene expression (Figure 2A). Our results showed a significant increase in PD-L1 gene expression in CD19<sup>-</sup>/138<sup>-</sup> cells in WM BM as compared with normal BM samples (Figure 2A top panel). The CD19<sup>+</sup>/138<sup>+</sup> cell population

had significantly higher PD-L1 and PD-L2 gene expression in the WM group as compared with normal counterparts; however, no significant difference was found for PD-1 expression (Figure 2A bottom panel). We then investigated tissue expression of these molecules on the BM sections using immunohistochemistry (IHC) staining (Figure 2B). IHC showed intense staining of both PD-L1 and PD-L2 on the BM sections, whereas slight PD-1 expression was detected. The intensity of the IHC staining for PD-L1 and PD-L2 appeared to be higher in WM BM compared with normal BM sections. To dissect which cell population could contribute to such an increased expression, we analyzed cell surface expression of these molecules on each distinct BM cell subpopulation involving CD19<sup>+</sup>/138<sup>+</sup> cells as well as CD19<sup>-</sup>/138<sup>-</sup> BM microenvironment cells; T-cell (CD3<sup>+</sup>), NK-cell (CD56<sup>+</sup>), monocyte (CD14<sup>+</sup>), and granulocyte (CD15<sup>+</sup>) populations (Figure 2C). Flow cytometry analysis showed surface expression of PD-L1 (Figure 2C), but rather minimal or undetectable PD-L2 expression (data not shown) on CD3<sup>+</sup>, CD14<sup>+</sup>, CD15<sup>+</sup>, and CD56<sup>+</sup> cell populations. T cells and monocytes within the WM CD19<sup>-</sup>/138<sup>-</sup> cell population contained significantly (*P* = .01) higher PD-L1 expression than their counterpart normal BM cells (Figure 2C). CD19<sup>+</sup>/138<sup>+</sup> WM cells showed modest expression of PD-L1 (Figure 2C) and PD-L2 (data not shown).

### Cytokine treatment increases soluble PD-L1 level in the media of the WM cell lines

We have shown that treatment of the WM cell lines with cytokines, including IL-21, IL-6, and IFN $\gamma$ , increases gene expression of PD-L1 and PD-L2 in MWCL-1 cells, and PD-L1 in the BCWM.1 cell line (Figure 1A-B), without detectable cytokine-induced PD-L1 surface expression, with an exception of IL-21-induced PD-L1 expression by BCWM.1 (Figure 1C). We next hypothesized that the lack or minimal cytokine-induced ligands surface expression by WM cell lines, despite increased gene expression, could be as a consequence of ligand cleavage and release into the microenvironment. To test this, we treated WM cell lines with 100 ng of IL-21, IFN $\gamma$ , CCL5, G-CSF or 50 ng/mL for 72 hours, collected cell-free-conditioned media and determined soluble PD-L1 and PD-L2 levels using an ELISA. As shown in Figure 3A, treatment with IL-21, IL-6, and IFN $\gamma$  increased PD-L1 levels in the media of both WM cell lines. It has been shown that PD-L1 expression can be induced in a JAK-STAT3-dependent manner in lung tumor cells.<sup>35</sup> Moreover, previous studies from our group indicate that IL-6 and IL-21 activate the JAK/STAT3 signaling pathway in the WM cells, thereby regulating biological effects, including IgM secretion, by these cells.<sup>14,16</sup> To explore whether the JAK/STAT3 pathway is also involved in IL-6- or IL-21-induced PD-L1 expression in WM cells, we treated BCWM.1 cell lines with IL-6 or IL-21, in the presence or absence of STAT3 inhibitor (STAT3 inhibitor) or CP690550 (JAK inhibitor), respectively, and measured the secreted PD-L1 level. Our data (Figure 3B) showed that inhibition of JAK or STAT3 reversed increased cytokine-mediated PD-L1 secretion, confirming that the activation of the JAK/STAT3 pathway mediates PD-L1 expression in WM.

### Soluble PD-L1 and PD-L2 levels are elevated in the BM plasma and peripheral serum of the WM patients compared with normal samples

The cytokine-induced elevation of soluble PD-L1 in the culture media of WM cell lines suggested that PD-1 ligands could also have the capacity to be released into the BM plasma and thereby into the circulating peripheral blood of the WM patients. To examine this, we



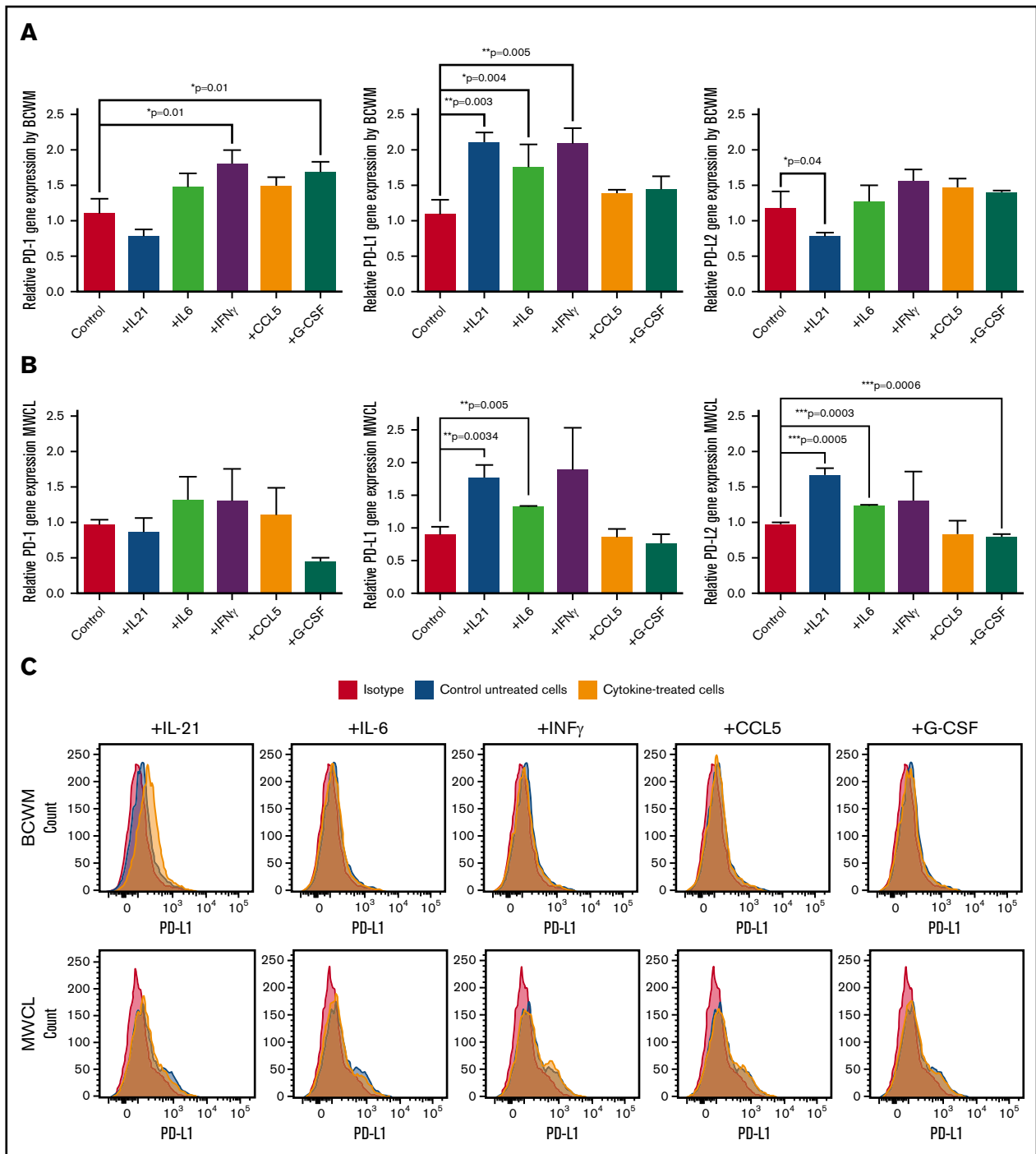


**Figure 1.** Effect of cytokine treatment on PD-1, PD-L1, and PD-L2 expression by BCWM.1 and MWCL-1 cell lines. BCWM.1 and MWCL-1 cell lines were starved overnight and then treated with complete media containing cytokines, including IL-21 (100 ng/mL), IL-6 (50 ng/mL), IFN $\gamma$  (100 ng/mL), CCL5 (100 ng/mL), and G-CSF (100 ng/mL) for 72 hours. (A-B) Cells were used for mRNA extraction, cDNA synthesis, and RT-PCR analysis. Bar graphs represent relative gene expression of PD-1, PD-L1, PD-L2 normalized to housekeeping gene (RPLPO) in response to cytokine treatment. Data are shown as the mean  $\pm$  SE of the mean (SEM) of 3 separate experiments ( $n = 3$ ). Significant differences and the  $P$  values are depicted on each graph. (C) Cells were stained with fluorochrome-conjugated anti-human PD-L1 antibody. Histograms represent flow cytometry analysis of PD-L1 surface expression by BCWM.1 and MWCL-1 cell lines (red, isotype control; blue, control untreated; and orange, cytokine-treated cells).

collected BM plasma and also peripheral blood serum samples from both WM patients and normal donors and performed an ELISA to detect PD-L1 and PD-L2 levels. As shown in Figure 4A, both BM

plasma and peripheral blood serum from WM patients contained higher levels of soluble PD-L1 and PD-L2, indicating that WM BM cells secrete the ligands into the tumor microenvironment.

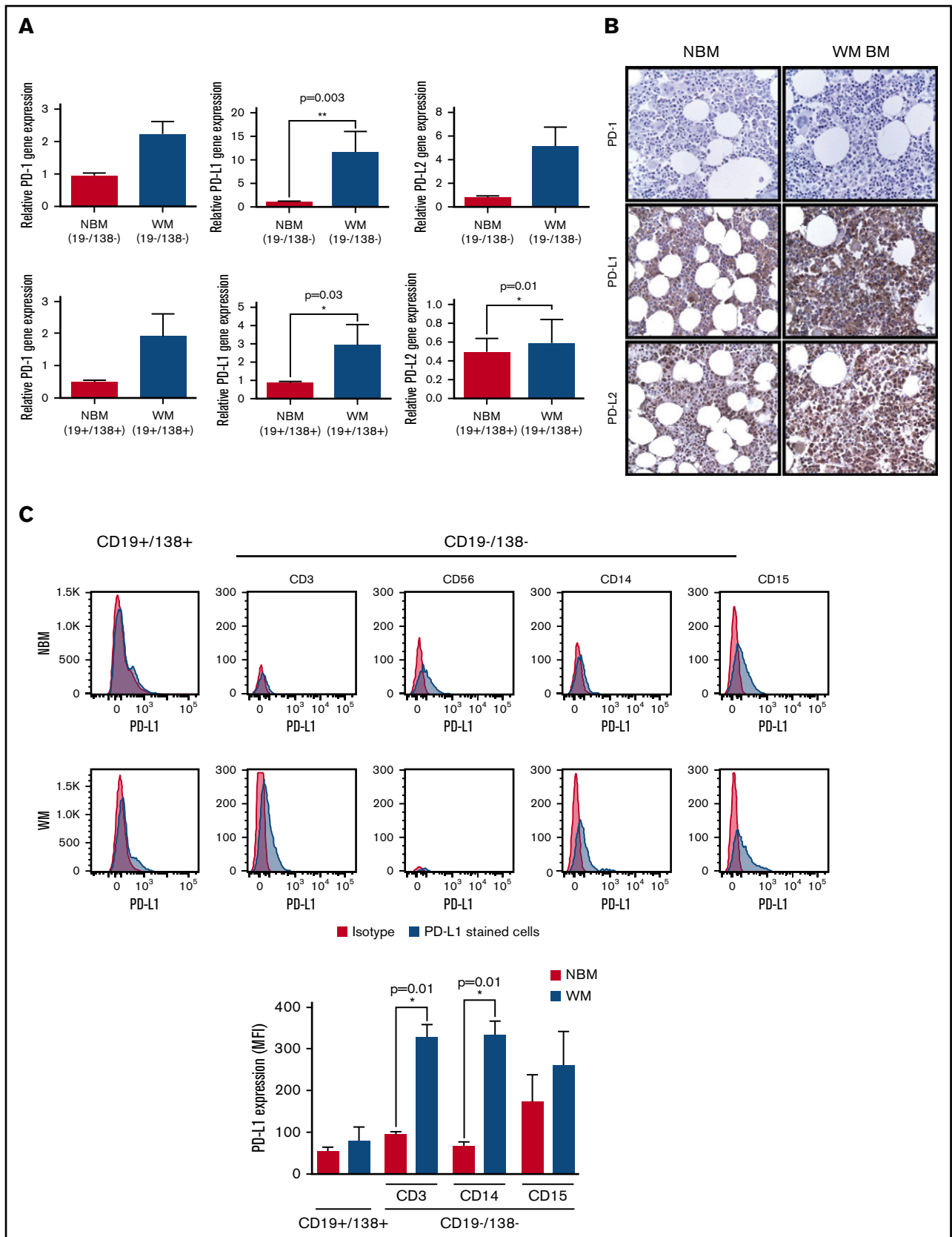


**Figure 2. PD-1, PD-L1, and PD-L2 expression in WM BM cells.** BM biopsies from WM patients were processed to isolate cells (CD19<sup>+</sup>/138<sup>+</sup> and CD19<sup>-</sup>/138<sup>+</sup>) and plasma fractions. Cells were used for RNA extraction, cDNA synthesis, and RT-PCR analysis. (A) Bar graphs represent relative gene expression of PD-1 and the ligands normalized to housekeeping gene; CD19<sup>-</sup>/138<sup>-</sup> (NBM, n = 9; WM, n = 18) and CD19<sup>+</sup>/138<sup>+</sup> (NBM, n = 8; WM, n = 15). Significant differences and related P values are shown on

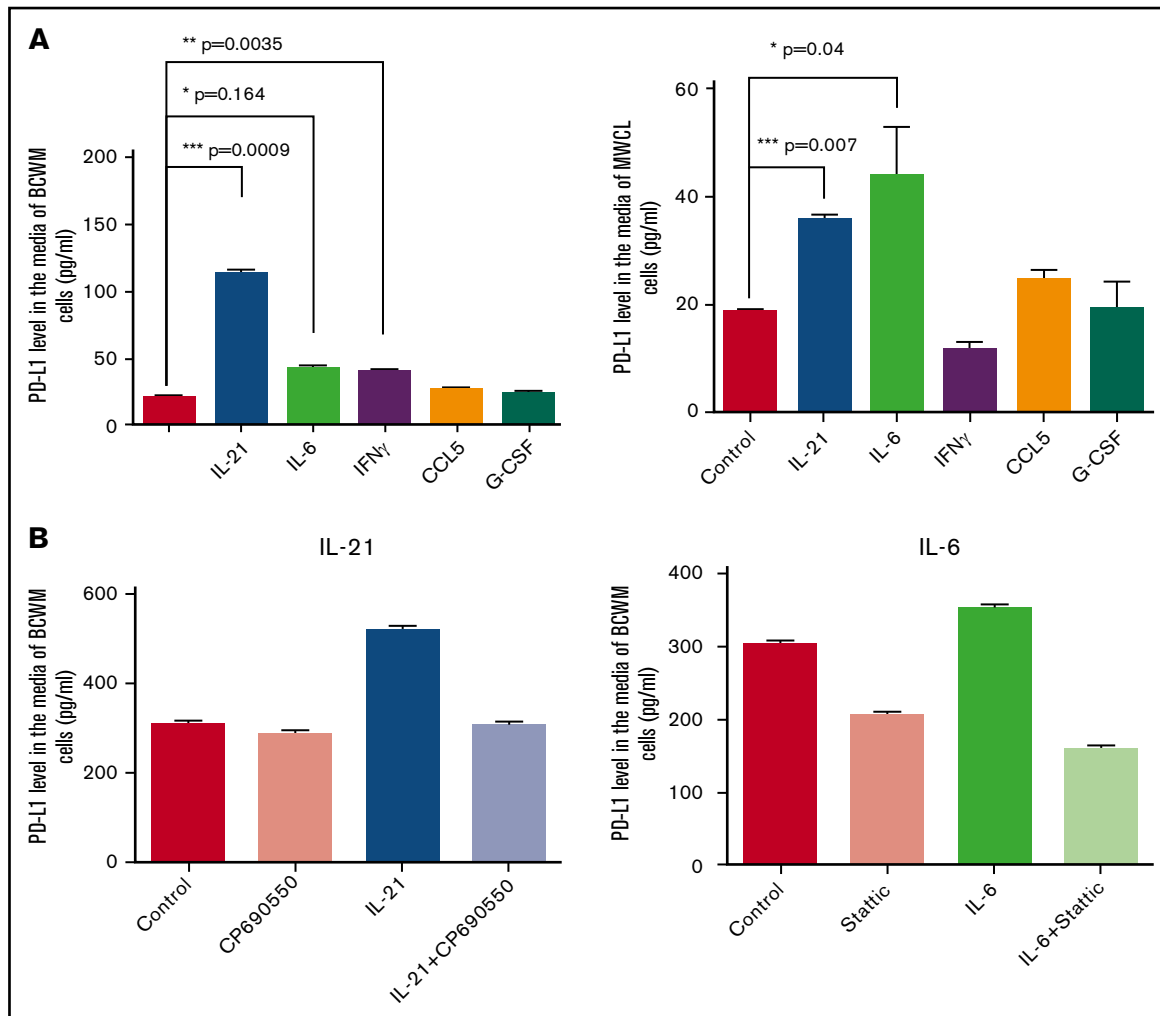


**Figure 3. Cytokine treatment increases soluble PD-L1 in the media of the WM cell lines.** BCWM.1 and MWCL-1 cells were treated with 100 ng/mL IL-21, IFN $\gamma$ , CCL5, G-CSF or 50 ng/mL IL-6 for 3 days. Media were collected and the level of soluble PD-L1 was determined using PD-L1 ELISA. (A) Bar graphs show the PD-L1 concentration (picograms per milliliter) in the media of the cells treated with cytokines. Data presented as mean  $\pm$  SEM of 3 individual experiments and significant differences are displayed on each graph. (B) Bar graph shows IL-21- or IL-6-induced PD-L1 secretion in BCWM.1 cells in the presence or absence of 1  $\mu$ M CP 690550 (left) and 0.5  $\mu$ M STATTIC (right).

We compared the level of PD-L1 or PDL2 in the BM plasma of patients with smoldering vs symptomatic WM, MYD88 wild-type vs MYD88<sup>L265P</sup> mutated and compared them with control normal BM (Figure 4B). Although each of these groups displayed significantly higher PD-L1 and PDL2 expression than normal samples, there were no significant differences among disease groups. Similarly, no significant differences were found between MYD88 wild-type vs MYD88<sup>L265P</sup> mutated disease status (Figure 4B).

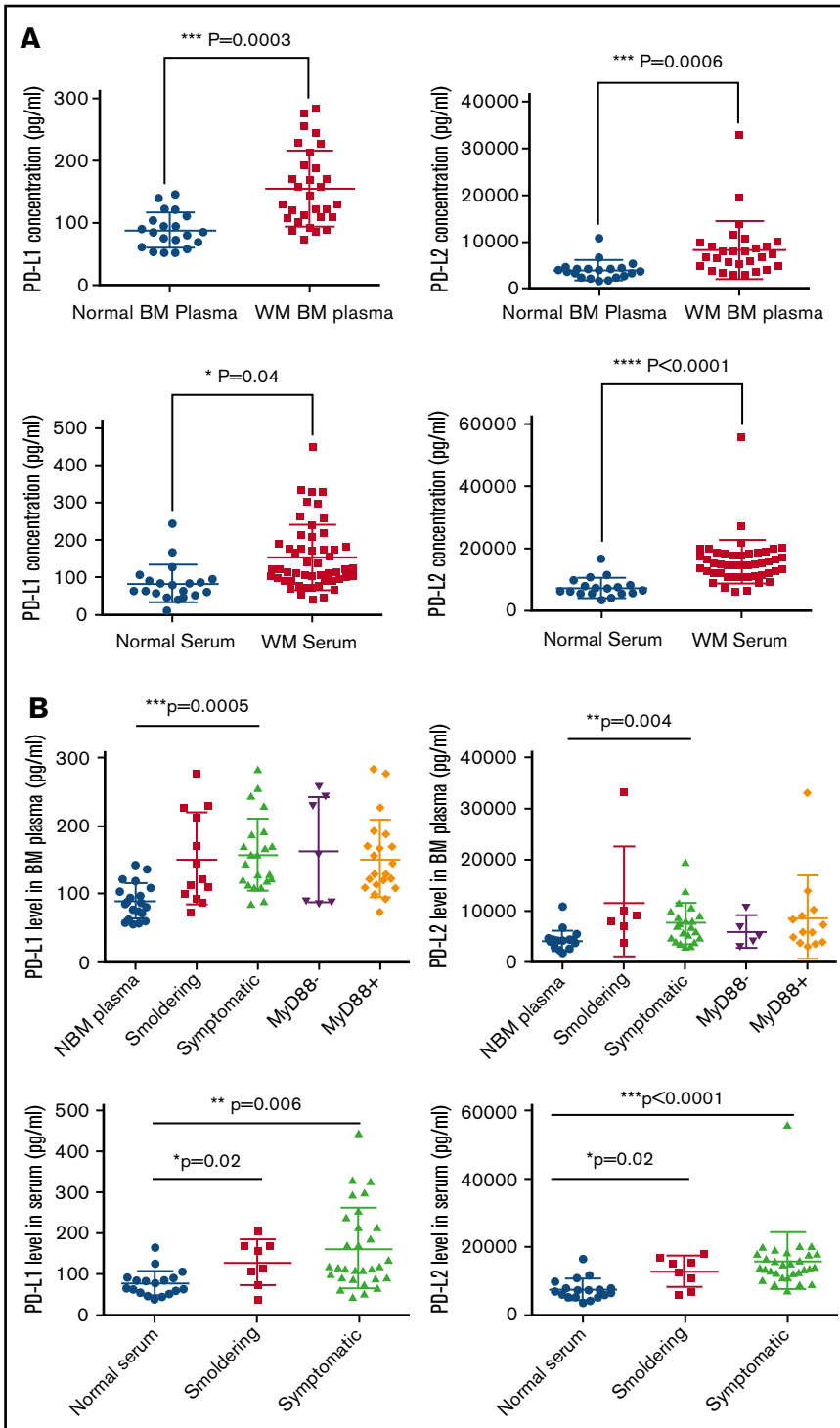
### Secretion of PD-L1 and PD-L2 by WM cells modulates T-cell function

To test the biological significance of soluble forms of PD-L1 and PD-L2, we generated WM cell lines overexpressing the ligands

using a lentiviral transfection system. The overexpression of the genes was verified by flow cytometry and the presence of soluble PD-L1 and PD-L2 was confirmed by western blot analysis on concentrated conditioned media collected from the transfected cells (Figure 5A). To assess the effect of soluble forms of PD-L1 and PD-L2 on T-cell function, we evaluated T-cell proliferation, cell cycle protein expression, and mitochondrial function in response to soluble forms of PD-L1 and PD-L2 secreted by WM cell lines. T cells were isolated from normal PBMCs and incubated with the conditioned media on OKT3-coated plates and in the presence of an anti-CD28 antibody to activate the cells for 3 days. Our data showed that addition of conditioned media containing either soluble PD-L1 or PD-L2 reduced the T-cell

**Figure 2. (continued)** each graph. (B) IHC staining shows the sections from WM and normal BM (NBM) stained for PD-1, PD-L1, and PD-L2 (brown stain; original magnification  $\times$ 400). (C) CD19<sup>+</sup>/138<sup>+</sup> and CD19<sup>-</sup>/138<sup>-</sup> cell populations were stained with PD-L1 and analyzed using flow cytometry. Histograms show PD-L1 surface expression on CD19<sup>+</sup>/138<sup>+</sup>, CD3<sup>+</sup>, CD56<sup>+</sup>, CD14<sup>+</sup> and CD15<sup>+</sup> cell fractions (isotype control [red] and PD-L1 [blue]) in WM and NBM. Bar graphs compare mean fluorescence intensity of 19<sup>+</sup>/138<sup>+</sup> cells between NBM and WM BM (NBM, n = 5; WM, n = 9). Data are presented as mean  $\pm$  SEM and significant differences and related P values are shown on each graph. MFI, mean fluorescence intensity.

**Figure 4. Level of soluble PD-L1 and PD-L2 concentration in the BM plasma as well as peripheral blood serum of the patients with WM.** Normal and WM BM samples were processed to separate cells from BM plasma containing soluble factors. Peripheral serum samples were collected from WM patients and normal donors. The concentration of PD-L1 and PD-L2 on these samples was determined using ELISA. (A) Dot plots compare mean  $\pm$  SEM of PD-L1 and PD-L2 between WM and normal samples. Normal BM plasma,  $n = 20$ ; WM plasma,  $n = 28$ ; normal serum,  $n = 20$ ; WM serum,  $n = 52$ . (B) Dot plots compare the PD-L1 and PD-L2 levels between normal, smoldering, and symptomatic WM patients, as well as MyD88<sup>-</sup> vs MyD88<sup>+</sup> WM patients. Significant differences and the  $P$  values are shown on each plot.



proliferation (Figure 5B). The reduction in T-cell proliferation was also associated with a decrease in the cell cycle protein cyclin A, as well as phosphorylated Akt (p-Akt) and p-ERK protein levels (Figure 5C). In additional experiments, T cells were stimulated with CD3/CD28 dynabeads for 3 days and then incubated with conditioned media. Soluble PD-L1 and PD-L2 could change the metabolic rate of T cells within 24 hours following T-cell

treatment, by reducing the maximal respiratory capacity of T cells and adenosine triphosphate production (Figure 5D). A similar effect was also observed 3 days following T-cell incubation with PD-L1 and PD-L2 (data not shown). These data indicated that increased soluble PD-L1 and PD-L2 in the BM plasma and peripheral circulation of WM patients can impact T-cell function at locations both close to and distant from tumor cells.



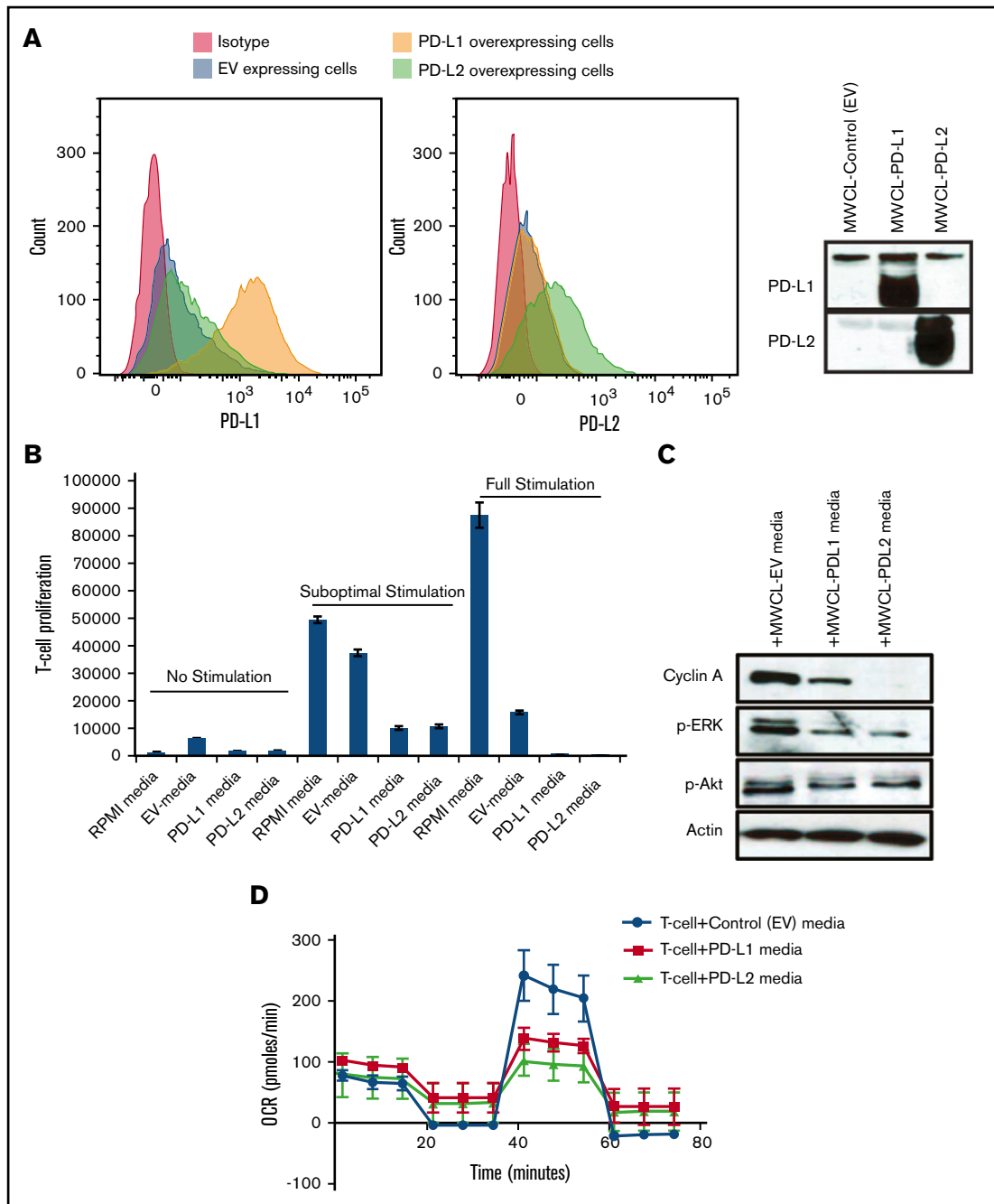


**Figure 5. T-cell incubation with the media secreted by WM cells overexpressing PD-L1 and PD-L2 reduces T-cell proliferation and cell cycle proliferation.** MWCL-1 cells were transfected with control EV, PD-L1, or PD-L2 constructs. (A) Histograms represent the flow cytometry analysis of the cells overexpressing either PD-L1 (left) or PD-L2 (right). Western blot analysis shows the overexpression of PD-L1 and PD-L2 on the cell surface and in the condition media of the cells, respectively. (B) T cells were isolated from PBMCs and incubated with cell-free media from MWCL-1 lines transfected with overexpressing PD-L1 or PD-L2 constructs. Cells were left either nonstimulated or stimulated with suboptimal (0.5  $\mu\text{g}/\text{mL}$ ) or optimal (5  $\mu\text{g}/\text{mL}$ ) dose of CD3 (0.5  $\mu\text{g}/\text{mL}$ ) and CD28. EV-transfected cells were used as control. Proliferation assay was performed using [ $^3\text{H}$ ]TdR following 72 hours of incubation. (C) Western blot analysis was performed on the T-cell lysates after 72 hours of incubation with the media from MWCL-1 lines. (D) Respiratory capacity of T cells in response to treatment with soluble PD-L1 and PD-L2. T cells were stimulated with CD3/CD28 dynabeads for 3 days, and then incubated with cell free-conditioned medias containing soluble PD-L1 and PD-L2 for 1 day. Respiratory capacity of T cells was measured using seahorse XFP analyzer. The diagram is a representative of 3 independent experiments.

## Discussion

The pathogenesis of WM is attributed not only to the genetic abnormalities in malignant cells but also to the impaired homeostasis of the BM microenvironment. The presence of a highly prevalent (>90%) somatic mutation in the MyD88 gene is shown to constitutively activate TLR pathways in a Bruton tyrosine kinase–dependent manner and results in increased survival and proliferation of the malignant cells. The significance of signaling through TLRs suggests that signals from the BM microenvironment remain important in regulating the growth of the malignant cells. It is, therefore, a necessity to explore novel mechanisms of WM pathogenesis. Here, we focused on studying the effect of the BM microenvironment on the immune checkpoint molecule, PD-1 and its ligands PD-L1 and PD-L2, and explored whether the altered cytokine secretion in the BM of WM could modulate these molecules, thereby controlling immune cell function, particularly T-cell function.

We have previously reported that chemokines and cytokines, including IL-6, G-CSF, CCL5, and IL-21, are elevated in the BM microenvironment of WM patients and contribute to increased WM cell proliferation and IgM secretion. In this study, we showed that these cytokines regulate gene expression of PD-1, PD-L1, and PD-L2. PD-1 and PD-L2 appear to be regulated in a cell-dependent manner, but the effect on the PD-L1 gene expression was similar between MWCL-1 and BCWM.1 (Figure 1A-B). Although both BCWM.1 and MWCL-1 cell lines represent WM disease characteristics and have been shown to express wild-type CXCR4 and mutant MyD88<sup>L265P</sup>,<sup>36</sup> they also differentially express several cell surface and intracellular markers that could explain the differential response to certain cytokines in this study.<sup>37-39</sup> The similar effect of cytokines on PD-L1 expression by 2 different cell lines indicates that there might be a common signaling mechanism regulating this pathway (Figure 1A-B). Increased IFN $\gamma$ -induced PD-L1 expression by tumor cells has been previously reported in oral squamous carcinoma and Hodgkin lymphoma and was shown to result in tumor-induced CD8<sup>+</sup> T-cell apoptosis.<sup>25,40</sup> Moreover, IFN $\gamma$ -induced PD-L1 expression has been shown to make tumor cells more resistant to cytotoxicity by NK cells.<sup>20</sup> It has also been shown that IL-21 also augments PD-L1 on T cells and antigen-presenting cells.<sup>21</sup> IL-6/JAK/STAT3 pathway is also shown to induce PD-L1 expression in epidermal growth factor–activated non–small cell lung cancer.<sup>41</sup>

In this study, we show that PD-L1 gene expression is significantly elevated in CD19<sup>+</sup>/138<sup>+</sup> and CD19<sup>-</sup>/138<sup>-</sup> cell populations isolated from WM patients (Figure 2A). This increase implies that changes in cytokine composition of the BM microenvironment in WM, including IL-21 and IL-6,<sup>14,16</sup> favor elevated levels of PD-L1. Increased PD-L1 expression by tumor cells is shown to induce T-cell exhaustion via interacting with its receptor PD-1 on T cells in several malignancies, including Hodgkin lymphoma.<sup>32,42</sup> Increased gene and surface expression of PD-L1 in the CD19/138<sup>-</sup> cell population, including T cells and monocytes (Figure 2C), supports the notion that the cells of the BM microenvironment play a role in the pathogenesis of WM. In Hodgkin lymphoma, CD163<sup>+</sup> monocytes/macrophages with high PD-L1 expression are shown to interact with PD-1<sup>hi</sup> NK cells and suppress their activity,<sup>43</sup> suggesting that the presence of PD-L1<sup>hi</sup> monocytes in WM could have biological significance. However, in WM samples, the number of NK cells was minimal or undetectable when compared with normal BM (Figure 2C), indicating another possible mechanism contributing to dysregulated WM tumor cell growth.

Despite increased gene expression, we could identify only very modest or negligible expression of PD-L1 or PD-L2 on the surface of CD19<sup>+</sup>/138<sup>+</sup> cells (Figure 2C). Similarly, cytokine-mediated cell surface PD-L1 expression was only detectable in BCWM.1 cells in response to IL-21, but not in other treatment settings (Figure 1C), suggesting that PD-L1 and/or PD-L2 are synthesized and subsequently cleaved and released to the tumor microenvironment. The analysis of patients samples confirmed PD-L1 and PD-L2 in soluble form in the BM plasma and also in the peripheral serum of WM patients, with concentrations significantly higher than their normal BM counterparts (Figure 4A). Consistently, treatment with IL-21, IL-6, and IFN $\gamma$  increased soluble PD-L1 levels in the media of the WM cell lines (Figure 3A), confirming the release of the soluble ligands into the microenvironment. Moreover, we showed that the effect of IL-6 and IL-21 on PD-L1 expression by BCWM.1 cells is mediated by the STAT3 and JAK pathway (Figure 3B). Previous work by our group has identified that IL-6 and IL-21 activate the JAK/STAT3 signaling pathway in WM cell lines and thereby transmit their biological effects by increasing IgM secretion.<sup>14,16</sup> Other studies also indicate that PD-L1 expression can be induced in a JAK-STAT3–dependent manner in tumor cells from lung cancer.<sup>35,41</sup> These data support our finding that IL-6– or IL-21–induced PD-L1 expression is mediated via the JAK/STAT3 pathway.

The presence of soluble PD-L1 and/or PD-L2 has been reported as prognostic biomarkers in several cancers. For instance, soluble PD-L1 shown to be elevated in the serum of the patients with NK/T-cell lymphoma,<sup>44</sup> pancreatic cancer,<sup>45</sup> non–small cell lung cancer,<sup>46</sup> diffuse large B-cell lymphoma,<sup>47</sup> and multiple myeloma.<sup>48</sup> The increased PD-L1 level in the serum of multiple myeloma patients is an indication of treatment response and progression-free survival.<sup>48,49</sup> Soluble PD-L1 from plasma of patients with non–small cell lung cancer is shown to have the ability to bind to PD-1.<sup>50</sup> A recent report indicates that mesenchymal stromal cells also secrete PD-1 ligands and modulate T-cell immunosuppressive activity.<sup>51</sup> Although we show that PD-L1 and PD-L2 levels are increased in WM and are biologically active, we did not test the prognostic impact of the serum levels on patient outcome. Future correlative studies using more WM specimens could address this hypothesis. Furthermore, secreted or circulating PD-L1 and PD-L2 can be found not only as soluble forms, but also conjugated with other proteins/molecules, or associated with exosomes or extracellular vesicles. Confirming this point, a very recent study has reported that PD-L1<sup>+</sup> exosomes are present in the plasma of the head and neck cancer patients and their levels correlate with disease progression.<sup>52</sup> The biological significance of exosome-mediated transfer of molecules has also been explored in WM, where exosome-packaged mutant MyD88<sup>L265P</sup> shown to activate the signaling of MyD88 wild-type cells.<sup>53</sup> Future studies are required to explore whether it is the soluble form, or exosome-associated PD-1 ligands that mediate biological effects of the ligands in our study.

Here, we explored the biological activity of soluble forms of PD-L1 and PD-L2 by generating stably transfected cells overexpressing the ligands. Using T cells isolated from PBMCs and the media of the overexpressing cell lines, we showed that soluble forms of PD-L1 and PD-L2 are able to diminish T-cell proliferation, cell cycle protein cyclin A, and cell survival signaling molecules p-Akt and p-ERK (Figure 5B-C). Furthermore, our data showed that soluble PD-L1 or PD-L2 could reduce adenosine triphosphate production and attenuate the respiratory capacity of T cells (Figure 5D). Mitochondrial respiratory capacity is a major factor regulating the memory development of

CD8 T cells<sup>54</sup> and associated with improved T-cell longevity<sup>55</sup> and support antigen-specific T-cell activation.<sup>56</sup> This is the first report indicating that the soluble PD-1 ligands are able to modulate T-cell metabolic function, and thereby contribute to T-cell inhibition. Although the focus of our study was to identify the biological significance of soluble ligands, membrane-bound PD-L1 and PD-L2 remain the important component of the BM microenvironment in WM, mediating the direct cell-to-cell interaction. In fact, membrane-bound ligands are shown to have strong inhibitory effect on T-cell function.<sup>57</sup>

In summary, we find that despite the presence of low PD-1 expression levels within the BM microenvironment, soluble PD-1 ligands present in the systemic circulation of the WM patients can biologically exert their function via systemic attenuation of T-cell function in distant locations, thereby potentially contributing to disease progression in WM. Based on the data presented in this study, therapeutic intervention using PD-L1 inhibitors, together with the agents that target malignant cells, could benefit patients with WM.

## Acknowledgments

The authors acknowledge the Mayo Clinic Center for Individualized Medicine for providing normal serum samples, and the

hematology clinical group and tumor bank for providing WM patients' samples.

This work was supported by the International Waldenstrom's Macroglobulinemia Foundation and Specialized Programs of Research Excellence in Lymphoma, National Institutes of Health, National Cancer Institute (P50 CA97274).

## Authorship

Contribution: S.J. designed and performed the experiments, and wrote the manuscript; T.P.-T. and H.-J.K. supported some laboratory work; J.P. and J.V. were involved in reviewing the patients' database; Z.-Z.Y. and A.J.N. were involved in editing the manuscript; and S.M.A. supervised the study and provided scientific input.

Conflict-of-interest disclosure: The authors declare no competing financial interests.

Correspondence: Shahrzad Jalali, Mayo Clinic, 200 First St SW, Rochester, MN 55905; e-mail: jalali.shahrzad@mayo.edu; and Stephen M. Ansell, Mayo Clinic, 200 First St SW, Rochester, MN 55905; e-mail: ansell.stephen@mayo.edu.

## References

1. Kasi PM, Ansell SM, Gertz MA. Waldenström macroglobulinemia. *Clin Adv Hematol Oncol*. 2015;13(1):56-66.
2. Monge J, Braggio E, Ansell SM. Genetic factors and pathogenesis of Waldenström's macroglobulinemia. *Curr Oncol Rep*. 2013;15(5):450-456.
3. Castillo JJ, Ghobrial IM, Treon SP. Biology, prognosis, and therapy of Waldenström macroglobulinemia. *Cancer Treat Res*. 2015;165:177-195.
4. Kapoor P, Ansell SM, Fonseca R, et al. Diagnosis and management of Waldenström macroglobulinemia: Mayo Stratification of Macroglobulinemia and Risk-Adapted Therapy (mSMART) guidelines 2016. *JAMA Oncol*. 2017;3(9):1257-1265.
5. Hunter ZR, Yang G, Xu L, Liu X, Castillo JJ, Treon SP. Genomics, signaling, and treatment of Waldenström macroglobulinemia. *J Clin Oncol*. 2017;35(9):994-1001.
6. Agarwal A, Ghobrial IM. The bone marrow microenvironment in Waldenström macroglobulinemia. *Clin Lymphoma Myeloma Leuk*. 2013;13(2):218-221.
7. Jalali S, Ansell SM. Bone marrow microenvironment in Waldenström's macroglobulinemia. *Best Pract Res Clin Haematol*. 2016;29(2):148-155.
8. Hunter ZR, Xu L, Yang G, et al. The genomic landscape of Waldenström macroglobulinemia is characterized by highly recurring MYD88 and WHIM-like CXCR4 mutations, and small somatic deletions associated with B-cell lymphomagenesis. *Blood*. 2014;123(11):1637-1646.
9. Poulain S, Roumier C, Venet-Caillault A, et al. Genomic landscape of CXCR4 mutations in Waldenström macroglobulinemia. *Clin Cancer Res*. 2016;22(6):1480-1488.
10. Treon SP, Xu L, Yang G, et al. MYD88 L265P somatic mutation in Waldenström's macroglobulinemia. *N Engl J Med*. 2012;367(9):826-833.
11. Yang G, Zhou Y, Liu X, et al. A mutation in MYD88 (L265P) supports the survival of lymphoplasmacytic cells by activation of Bruton tyrosine kinase in Waldenström macroglobulinemia. *Blood*. 2013;122(7):1222-1232.
12. Cao Y, Hunter ZR, Liu X, et al. The WHIM-like CXCR4(S338X) somatic mutation activates AKT and ERK, and promotes resistance to ibrutinib and other agents used in the treatment of Waldenström's macroglobulinemia. *Leukemia*. 2015;29(1):169-176.
13. Elsawa SF, Ansell SM. Cytokines in the microenvironment of Waldenström's macroglobulinemia. *Clin Lymphoma Myeloma*. 2009;9(1):43-45.
14. Elsawa SF, Novak AJ, Ziesmer SC, et al. Comprehensive analysis of tumor microenvironment cytokines in Waldenström macroglobulinemia identifies CCL5 as a novel modulator of IL-6 activity. *Blood*. 2011;118(20):5540-5549.
15. Hatzimichael EC, Christou L, Bai M, Kolios G, Kefala L, Bourantas KL. Serum levels of IL-6 and its soluble receptor (sIL-6R) in Waldenström's macroglobulinemia. *Eur J Haematol*. 2001;66(1):1-6.
16. Hodge LS, Ziesmer SC, Yang ZZ, et al. IL-21 in the bone marrow microenvironment contributes to IgM secretion and proliferation of malignant cells in Waldenström macroglobulinemia. *Blood*. 2012;120(18):3774-3782.
17. Terpos E, Anagnostopoulos A, Kastritis E, Bamias A, Tsioukas K, Dimopoulos MA. Abnormal bone remodelling and increased levels of macrophage inflammatory protein-1 alpha (MIP-1 alpha) in Waldenström macroglobulinemia. *Br J Haematol*. 2006;133(3):301-304.
18. Terpos E, Tasidou A, Eleftherakis-Papaiakovou E, et al. Expression of CCL3 by neoplastic cells in patients with Waldenström's macroglobulinemia: an immunohistochemical study in bone marrow biopsies of 67 patients. *Clin Lymphoma Myeloma Leuk*. 2011;11(1):115-117.
19. Elsawa SF, Novak AJ, Grote DM, et al. B-lymphocyte stimulator (BLyS) stimulates immunoglobulin production and malignant B-cell growth in Waldenström macroglobulinemia. *Blood*. 2006;107(7):2882-2888.

20. Bellucci R, Martin A, Bommarito D, et al. Interferon- $\gamma$ -induced activation of JAK1 and JAK2 suppresses tumor cell susceptibility to NK cells through upregulation of PD-L1 expression. *Oncol Immunology*. 2015;4(6):e1008824.
21. Kinter AL, Godbout EJ, McNally JP, et al. The common gamma-chain cytokines IL-2, IL-7, IL-15, and IL-21 induce the expression of programmed death-1 and its ligands. *J Immunol*. 2008;181(10):6738-6746.
22. Ok CY, Young KH. Checkpoint inhibitors in hematological malignancies. *J Hematol Oncol*. 2017;10(1):103.
23. Thanarajasingam G, Thanarajasingam U, Ansell SM. Immune checkpoint blockade in lymphoid malignancies. *FEBS J*. 2016;283(12):2233-2244.
24. Riley JL. PD-1 signaling in primary T cells. *Immunol Rev*. 2009;229(1):114-125.
25. Green MR, Monti S, Rodig SJ, et al. Integrative analysis reveals selective 9p24.1 amplification, increased PD-1 ligand expression, and further induction via JAK2 in nodular sclerosing Hodgkin lymphoma and primary mediastinal large B-cell lymphoma. *Blood*. 2010;116(17):3268-3277.
26. Fourcade J, Sun Z, Benallaoua M, et al. Upregulation of Tim-3 and PD-1 expression is associated with tumor antigen-specific CD8+ T cell dysfunction in melanoma patients. *J Exp Med*. 2010;207(10):2175-2186.
27. Hino R, Kabashima K, Kato Y, et al. Tumor cell expression of programmed cell death-1 ligand 1 is a prognostic factor for malignant melanoma. *Cancer*. 2010;116(7):1757-1766.
28. Prado-Garcia H, Romero-Garcia S, Puerto-Aquino A, Rumbo-Nava U. The PD-L1/PD-1 pathway promotes dysfunction, but not "exhaustion", in tumor-responding T cells from pleural effusions in lung cancer patients. *Cancer Immunol Immunother*. 2017;66(6):765-776.
29. Muenst S, Schaerli AR, Gao F, et al. Expression of programmed death ligand 1 (PD-L1) is associated with poor prognosis in human breast cancer. *Breast Cancer Res Treat*. 2014;146(1):15-24.
30. Hamanishi J, Mandai M, Iwasaki M, et al. Programmed cell death 1 ligand 1 and tumor-infiltrating CD8+ T lymphocytes are prognostic factors of human ovarian cancer. *Proc Natl Acad Sci USA*. 2007;104(9):3360-3365.
31. Nakanishi J, Wada Y, Matsumoto K, Azuma M, Kikuchi K, Ueda S. Overexpression of B7-H1 (PD-L1) significantly associates with tumor grade and postoperative prognosis in human urothelial cancers. *Cancer Immunol Immunother*. 2007;56(8):1173-1182.
32. Ansell SM, Lesokhin AM, Borrello I, et al. PD-1 blockade with nivolumab in relapsed or refractory Hodgkin's lymphoma. *N Engl J Med*. 2015;372(4):311-319.
33. Xia B, Herbst RS. Immune checkpoint therapy for non-small-cell lung cancer: an update. *Immunotherapy*. 2016;8(3):279-298.
34. Zhu X, Lang J. Programmed death-1 pathway blockade produces a synergistic antitumor effect: combined application in ovarian cancer. *J Gynecol Oncol*. 2017;28(5):e64.
35. Zhang X, Zeng Y, Qu Q, et al. PD-L1 induced by IFN- $\gamma$  from tumor-associated macrophages via the JAK/STAT3 and PI3K/AKT signaling pathways promoted progression of lung cancer. *Int J Clin Oncol*. 2017;22(6):1026-1033.
36. Xu L, Tsakmaklis N, Yang G, et al. Acquired mutations associated with ibrutinib resistance in Waldenström macroglobulinemia. *Blood*. 2017;129(18):2519-2525.
37. Ditzel Santos D, Ho AW, Tournilhac O, et al. Establishment of BCWM.1 cell line for Waldenström's macroglobulinemia with productive in vivo engraftment in SCID-hu mice. *Exp Hematol*. 2007;35(9):1366-1375.
38. Hodge LS, Novak AJ, Grote DM, et al. Establishment and characterization of a novel Waldenström macroglobulinemia cell line, MWCL-1. *Blood*. 2011;117(19):e190-e197.
39. Paulus A, Chitta KS, Wallace PK, et al. Immunophenotyping of Waldenström's macroglobulinemia cell lines reveals distinct patterns of surface antigen expression: potential biological and therapeutic implications. *PLoS One*. 2015;10(4):e0122338.
40. Chen J, Feng Y, Lu L, et al. Interferon- $\gamma$ -induced PD-L1 surface expression on human oral squamous carcinoma via PKD2 signal pathway. *Immunobiology*. 2012;217(4):385-393.
41. Zhang N, Zeng Y, Du W, et al. The EGFR pathway is involved in the regulation of PD-L1 expression via the IL-6/JAK/STAT3 signaling pathway in EGFR-mutated non-small cell lung cancer. *Int J Oncol*. 2016;49(4):1360-1368.
42. Goodman A, Patel SP, Kurzrock R. PD-1-PD-L1 immune-checkpoint blockade in B-cell lymphomas. *Nat Rev Clin Oncol*. 2017;14(4):203-220.
43. Vari F, Arpon D, Keane C, et al. Immune evasion via PD-1/PD-L1 on NK cells and monocyte/macrophages is more prominent in Hodgkin lymphoma than DLBCL. *Blood*. 2018;131(16):1809-1819.
44. Nagato T, Ohkuri T, Ohara K, et al. Programmed death-ligand 1 and its soluble form are highly expressed in nasal natural killer/T-cell lymphoma: a potential rationale for immunotherapy. *Cancer Immunol Immunother*. 2017;66(7):877-890.
45. Kruger S, Legenstein ML, Rösger V, et al. Serum levels of soluble programmed death protein 1 (sPD-1) and soluble programmed death ligand 1 (sPD-L1) in advanced pancreatic cancer. *Oncol Immunology*. 2017;6(5):e1310358.
46. Xing YF, Zhang ZL, Shi MH, Ma Y, Chen YJ. The level of soluble programmed death-1 in peripheral blood of patients with lung cancer and its clinical implications [in Chinese]. *Zhonghua Jie He He Hu Xi Za Zhi*. 2012;35(2):102-106.
47. Rossille D, Gressier M, Damotte D, et al; Groupe Ouest-Est des Leucémies et Autres Maladies du Sang. High level of soluble programmed cell death ligand 1 in blood impacts overall survival in aggressive diffuse large B-cell lymphoma: results from a French multicenter clinical trial. *Leukemia*. 2014;28(12):2367-2375.
48. Wang L, Wang H, Chen H, et al. Serum levels of soluble programmed death ligand 1 predict treatment response and progression free survival in multiple myeloma. *Oncotarget*. 2015;6(38):41228-41236.
49. Huang SY, Lin HH, Lin CW, et al. Soluble PD-L1: a biomarker to predict progression of autologous transplantation in patients with multiple myeloma. *Oncotarget*. 2016;7(38):62490-62502.

50. Takeuchi M, Doi T, Obayashi K, et al. Soluble PD-L1 with PD-1-binding capacity exists in the plasma of patients with non-small cell lung cancer. *Immunol Lett.* 2018;196:155-160.
51. Davies LC, Heldring N, Kadri N, Le Blanc K. Mesenchymal stromal cell secretion of programmed death-1 ligands regulates T cell mediated immunosuppression. *Stem Cells.* 2017;35(3):766-776.
52. Theodoraki MN, Yerneni SS, Hoffmann TK, Gooding WE, Whiteside TL. Clinical significance of PD-L1+ exosomes in plasma of head and neck cancer patients. *Clin Cancer Res.* 2018;24(4):896-905.
53. Manček-Keber M, Lainšček D, Benčina M, et al. Extracellular vesicle-mediated transfer of constitutively active MyD88L265P engages MyD88wt and activates signaling. *Blood.* 2018;131(15):1720-1729.
54. van der Windt GJ, Everts B, Chang CH, et al. Mitochondrial respiratory capacity is a critical regulator of CD8+ T cell memory development. *Immunity.* 2012;36(1):68-78.
55. Menk AV, Scharping NE, Rivadeneira DB, et al. 4-1BB costimulation induces T cell mitochondrial function and biogenesis enabling cancer immunotherapeutic responses. *J Exp Med.* 2018;215(4):1091-1100.
56. Leavy O. T cells: mitochondria and T cell activation. *Nat Rev Immunol.* 2013;13(4):224.
57. Patel SP, Kurzrock R. PD-L1 expression as a predictive biomarker in cancer immunotherapy. *Mol Cancer Ther.* 2015;14(4):847-856.